Residual Equinus After the Ponseti Method: An MRI-based 3-Dimensional Analysis

Joseph Mitchell, MD, Aaron Bishop, BS,† Yixuan Feng, MS,‡ Daniel Farley, MS,‡ Scott Hetzel, MS,* Heidi-Lynn Ploeg, PhD,†‡ Jie Nguyen, MS, MD,* and Kenneth J. Noonan, MD**

Background: Residual equinus deformity is present in up to 20% of clubfeet treated by the Ponseti method. These patients may require surgical release to restore dorsiflexion. Despite complete posterior release; persistent intraoperative equinus may be present and suggest concurrent joint incongruity. The purpose of this study was to characterize differences in ankle morphology in toddlers with residual equinus following the Ponseti method.

Methods: Preoperative magnetic resonance imaging (MRI) data from 10 patients who underwent reconstruction (17 feet; 7 bilateral, 3 unilateral clubfeet) for persistent equinus were compared with 16 age-matched controls. Through reverse engineering software, MRI data were used to generate 3-dimensional (3D) models. Four talus-based measures were performed on both MRI data and 3D models —neck depth, neck angle, width, and length. Models were also used to calculate talus volume and arc of curvature (plafond and talar dome). Standard statistical analyses were performed.

Results: Talus volumes, width, and length were less in clubfeet then in control feet. Although some measures were significant there was no mismatch with the ankle mortise dimensions or arc curvature that could account for any decrease in dorsiflexion. We found that from MRI measures the clubfoot neck depth was 2.3 versus 3.6 mm in controls ($P < 0.001$) and from 3D modeling the clubfoot neck depth was 2.3 and 3.5 mm in controls ($P = 0.003$). With 3D modeling talus clubfoot neck angle was 153.7 versus 140.4 degrees in controls ($P = 0.01$). The clubfoot neck angle obtained from MRI measures were also different yet not significant [126.6 in clubfeet versus 122.5 degrees in controls ($P = 0.12$)].

Conclusions: In comparison to age-matched feet; we have noted a decrease in talar neck depth and an obtuse talar neck angle in clubfeet treated in the manner of Ponseti. This may result in anterior ankle impingement and be the cause of residual equinus despite posterior release. In these procedures, the surgeon should recognize this possibility when the amount of dorsiflexion is less than expected.

From the *Department of Orthopedics and Rehabilitation, University of Wisconsin School of Medicine and Public Health; Departments of ‡ Mechanical Engineering; and †Biomedical Engineering, College of Engineering, University of Wisconsin-Madison, Madison, WI.

No authors received anything of monetary value for this research.
The authors declare no conflicts of interest.

Reprints: Kenneth J. Noonan, MD, 1685 Highland Avenue, Room 6264, Madison, WI 53705. E-mail: noonan@ortho.wisc.edu.

DOI: 10.1097/BPO.0000000000001147

Level of Evidence: Level III—case control study.

Key Words: clubfoot, talus, modeling, deformity, idiopathic talipes equinovarus, magnetic resonance imaging

(*J Pediatr Orthop* 2018;00:000–000)

Residual equinus deformity is present in up to 20% of clubfeet treated by the Ponseti method of serial casting and percutaneous tenotomy.[1] In addition, recurrence rates have been reported as high as 20% to 40% in a recent survey of practicing pediatric orthopaedists.[2] These patients with residual or recurrent deformity will require further treatment, which may ultimately lead to surgical intervention to restore dorsiflexion. Surgical release for residual equinus deformity in toddlers with clubfoot is usually a stepwise progression. Surgical methodology begins with tendoachilles lengthening. Further surgical steps may be considered to gain additional dorsiflexion, including posterior ankle and subtalar joint release. If persistent equinus is present; it is possible that the ankle mortise is narrowed in relation to the wider anterior talar body and that further release of the tibiofibular syndesmosis could accommodate further dorsiflexion. Despite surgical release of all posterior structures, a subset of these patients will have persistent equinus intraoperatively and may be suggestive of underlying bony or cartilaginous ankle incongruity.

Attempts to characterize bony morphology in the older clubfoot have been performed via radiographic, computed tomography (CT), and cadaver-based studies.[3–7] Through the aforementioned studies, multiple differences exist in the clubfoot ankle. The clubfoot talus has been described as flat topped and hypoplastic, with medial and plantar deviation of the head and neck.[8–14] In recent years, magnetic resonance (MRI)-based studies have become available and may be preferable in younger patients given the predominance of cartilage in this population and the desire to minimize radiation. The purpose of this study was to use MRI to characterize differences in ankle morphology in toddlers who had residual equinus deformity after the Ponseti method. In particular, we aimed to determine if ankle morphology incongruences (eg, flat top talus, narrowed mortise width or signs of talar impingement) could account for residual equinus.

METHODS

Patient Population

We collected a series of 10 consecutive patients who underwent reconstruction for persistent clubfoot deformity that included residual equinus (Table 1). Standard Institutional Review Board approval was obtained before starting the study. Before surgery, all clubfoot patients were treated with serial Ponseti casting (for an average of 6.0 wk), with percutaneous tenotomy and had use of foot abduction orthosis for an average of 2.7 years (0.06 to 5.0 y). The decision to proceed with surgery was made clinically based on physical examination with a preoperative average forced dorsiflexion of only 1 degree. As part of their preoperative evaluation, each child had an MRI of the ankle and hindfoot of both feet under general sedation. Forced dorsiflexion via casting or alternative methods was not attempted. MRI studies were performed utilizing a 3.0 Telsa scanner, producing both T1-weighted and T2-weighted images of 3 to 4 mm slice thickness. Each study was assessed with standard coronal, sagittal, and axial planes.

To detect articular incongruities as a potential source of diminished dorsiflexion, preoperative MRI data from the 10 clubfoot patients (17 total ankles; 7 bilateral cases, 3 unilateral cases) with an average age of 4.7 years were compared with 16 age-matched controls (average age of 4.8 y, $P = 0.63$). The control group MRIs were obtained for a variety of clinical reasons, however none had a history of clubfoot or other congenital foot conditions. Control MRIs were predominantly obtained to investigate complaints of ankle and/or foot pain, which accounted for 54% of the listed indications. Additional reasons included soft tissue masses (31%) and surveillance (15%). Thirty-six percent of applicable (ie, nonsurveillance) studies were interpreted as normal. Diagnoses of fibular osteomyelitis (21%), vascular anomalies (21%), lipoma, Kohler disease, synovitis, and cellulitis were rendered in the remaining cases. To increase our sample of control patients; in the case of our 3 unilateral clubfoot subjects, their contralateral normal ankle was included in the control cohort.

Three-dimensional (3D) Model Generation

The process of 3D model generation began with raw MRI data. Using the software package Mimics version 17 (Materialise, Leuven, Belgium) each scan was segmented to create "masks" of the talus, tibia, and fibula. For each ankle, 3 sets of masks were generated utilizing a different anatomic plane to convert 2D data into 3D. For example, axial images in the *XY* (transverse) plane were used to make masks in the *XZ* (coronal) and *YZ* (sagittal) planes. These masks were then exported as stereolithographic (stl) files into the reverse engineering software package Geomagic Studio (3D Systems, Rock Hill, SC) for further processing.

Once the stl files were transitioned into the Geomagic software they were merged to produce unprocessed models of each individual bone. The models were then manually and globally registered to align anatomic landmarks and minimize deviation between surfaces. Following the alignment, a mesh wrap was generated using the best surfaces of all models and a final surface was created from the aforementioned mesh to produce the complete stl model. This process allowed for the generation of a 3D model with the best possible surface resolution and accuracy with the given MRI data. In order to access ankle morphology; we assessed the ankle by direct picture archiving and communication

TABLE 1. Surgical Interventions to Address Residual Deformity Within the Clubfoot Cohort

Patient	Laterality	Age (y)	MRI Talar Neck Depth (mm)	Preoperative Dorsiflexion (deg.)	Procedure
1	R	2.1	2.9	0	Achilles tenotomy, ATT transfer
2a	R	5.0	2.4	0	ATT transfer, midfoot osteotomy, plantar fascia release, posterior release
2b	L	5.0	2.3	5	Achilles tenotomy, ATT transfer
3	R	6.2	2.1	−10	Medial release, metatarsal osteotomies, midfoot osteotomy, plantar fascia release, posterior release
4a	R	5.2	1.8	0	ATT transfer, midfoot osteotomy, plantar fascia release, posterior release
4b	L	5.2	1.8	0	Achilles lengthening, ATT transfer, midfoot osteotomy, posterior release
5a	R	5.6	2.9	0	Achilles lengthening, ATT transfer, midfoot osteotomy, plantar fascia release, posterior release
5b	L	5.6	3.6	10	Achilles lengthening, ATT transfer, midfoot osteotomy
6a	R	4.2	2.6	NA	ATT transfer, midfoot osteotomy, posterior release
6b	L	4.2	2.5	10	Achilles lengthening, ATT transfer
7	L	5.0	2.2	0	Achilles lengthening, ATT transfer
8a	R	6.0	2.0	0	Achilles lengthening, ATT transfer, posterior release
8b	L	6.0	1.8	10	Achilles lengthening, midfoot osteotomy, posterior release
9a	R	5.1	2.7	0	Achilles lengthening, ATT transfer
9b	L	5.1	2.6	0	Achilles lengthening, ATT transfer, midfoot osteotomy, plantar fascial release, posterior release
10a	R	2.3	1.9	−5	Achilles lengthening, ATT transfer, posterior release
10b	L	2.3	1.6	−5	Achilles lengthening, ATT transfer, posterior release

Posterior release implies capsular release +/− release of the syndesmosis. Midfoot osteotomies were lateral column shortening osteotomies.
ATT indicates anterior tibialis tendon; L, left; MRI, magnetic resonance imaging; NA, not available; R, right.

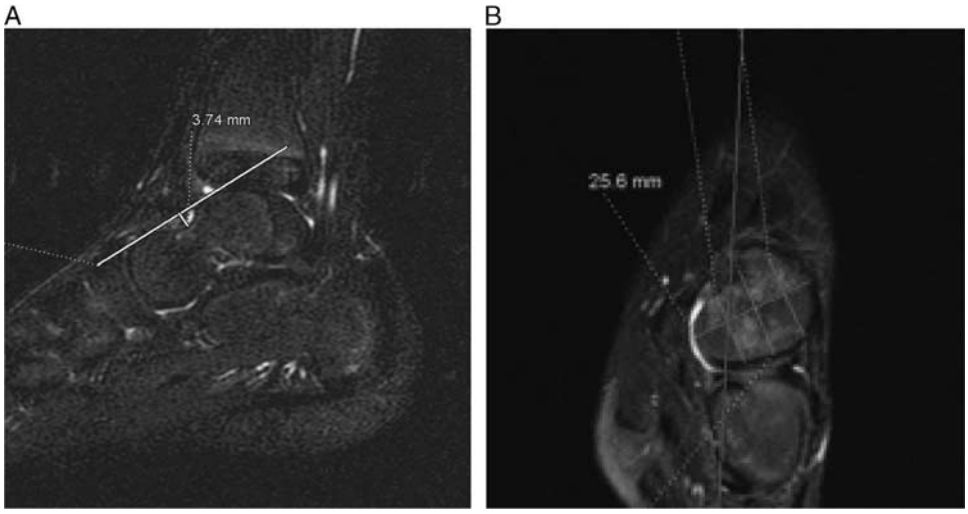

FIGURE 1. Talar neck depth. A, Distance from the deepest portion of the talar neck to a perpendicular line spanning the talar dome and head. B, We began by measuring the length of the talar neck in the coronal plane. This length was divided by 4 to generate 3 equidistant points. Neck angle and depth measures were then made as close as possible to each point dependent on slice thickness and orientation.

system (PACS) measures of MRI images as well as measures taken from computer generated 3D models.

MRI Measures

Four talus measures were obtained directly from PACS including neck depth, neck angle, width, and length. Neck depth (Fig. 1) was defined as the distance from the deepest portion of the talar neck to a perpendicular line spanning across from the talar dome to the talar head. The deepest point of the talar neck also served as the vertex for the neck angle (Fig. 2), with anterior and posterior arms along the head and talar dome, respectively. All of the measurements involving the talar neck were obtained at 3 equidistant "reference points" across the neck and averaged to eliminate measurement point variation between subjects. The particular slice used for measurement was that which fell in closest proximity to the previously determined reference points. Talar width (Fig. 3A) was defined as the distance across the body of the talus between the articulating surfaces of the tibia and fibula. Mortise width was simply an extension of the talus width measurement to abut the articular cartilage of the medial and lateral malleolus (Fig. 3B). These measures were obtained at the superior articular surface, the tip of the medial malleolus, and the midpoint between the 2. Length was defined as the distance from the most distal portion of the talar head to the tip of the posterior tubercle of the talus. Each of these measures were performed by both a pediatric musculoskeletal radiologist and an orthopaedic resident with excellent agreement (see below).

3D model measurements followed an identical protocol for assessment of talus neck depth, neck angle, width, and length. It should be noted that the location of our reference

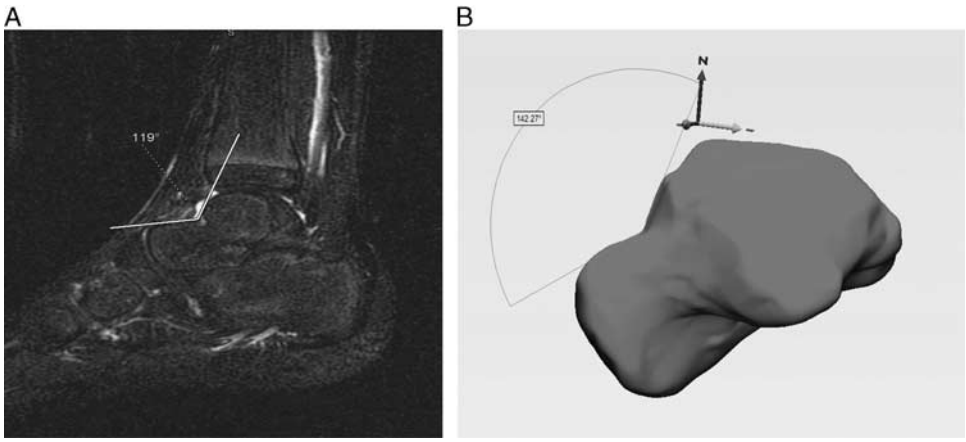

FIGURE 2. Talar neck angle—centered at the talar neck with anterior and posterior arms placed along the talar head and body, respectively. The neck angle was assessed at the same points as the talar neck depth and also averaged. A, PACS-based measurement. B, Model-based measurement. PACS indicates picture archiving and communication system.

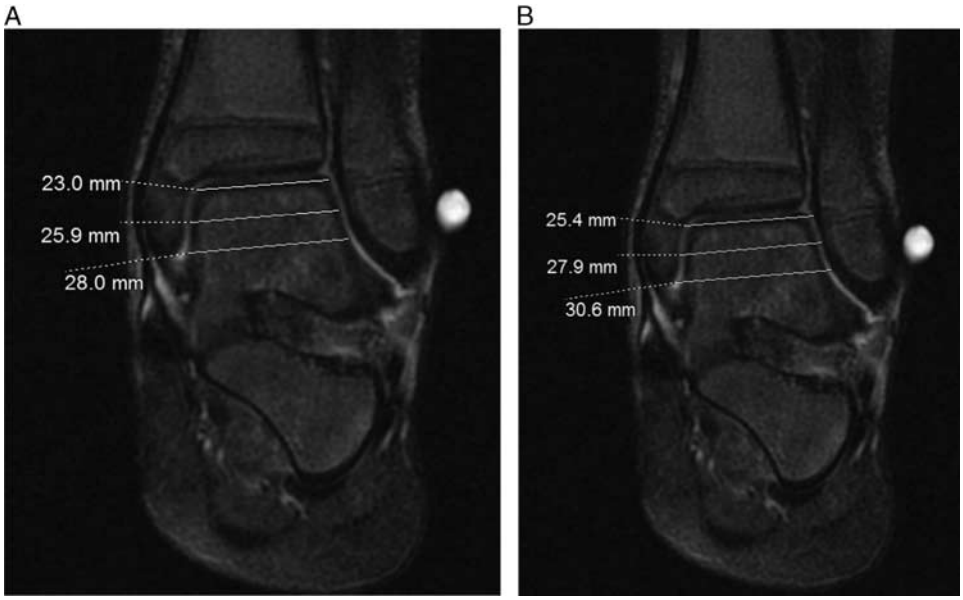

FIGURE 3. Talus width—distance across the body of the talus between the tibial and fibular articulating surfaces. This was measured at predetermined reference points and also at the site of maximum width (A). Mortise width—distance between the articulating surfaces of the medial and lateral malleoli. Measured at the same reference points as talar width (B).

point dependent measures (ie, neck depth, angle) did vary when compared with PACS. When assessing the 3D models, the location of these measurements was more standard as slice thickness was irrelevant. Additional model specific parameters included volume as well as tibial and talar dome arc of curvature. Talus volume was automatically calculated by the 3-Matic program once the talus models were loaded into the software. Arc of curvature was calculated at the previously described reference points for determining talar neck angle and depth. Circles were then fit to match the superior surface of the talar dome and the inferior surface of the tibial plafond. The radii of these circles were reported as arc of curvature in millimeters.

Statistical Analysis

The patient population in this study (and resultant database) was complex with 7 cases of bilateral clubfeet as well as 3 unilateral cases that contributed to both the control and clubfoot cohorts. To account for this, we examined differences between groups while controlling for laterality and modeling the variability of repeated measures from the 2 reviewers and within each subject. Multivariate repeated measures analysis of variance (RM-ANOVA) testing was utilized to compare groups controlling for laterality and age as fixed effects. Univariate RM-ANOVA was utilized to look for differences between groups not controlling for side with the patient nested within the reviewer as random effect.

RESULTS

PACS Measures

Direct cross-sectional data measurements revealed talus widths of 23.2 versus 25.3 mm in clubfoot and control cohorts, respectively ($P = 0.006$). Mortise width was also significantly smaller within the clubfoot group at 26.0 mm compared with 27.5 mm in controls ($P = 0.027$). A mortise to talus ratio was subsequently calculated and determined to be 1.13 in clubfoot ankles and 1.09 in controls ($P = 0.017$). Length of clubfoot and control tali was similar at 42.0 and 43.1 mm, respectively ($P = 0.303$). The average neck depth in clubfeet was 2.3 mm while that of controls was significantly deeper at 3.6 mm ($P < 0.001$). Clubfoot neck angles approached significance, but remained comparable at 126.6 degrees with 122.5 degrees found in age-matched controls ($P = 0.116$).

There was great interobserver reliability for all PACS measures, which is reported in Table 2. All interobserver

TABLE 2. Results of PACS-based Measurements Along With Significance and Interobserver Reliability Reported Using ICC

Variables	Group	Mean (95% CI)	*P*	Interobserver ICC
Talus width	Clubfoot	23.2 (15.6, 30.8)	0.006	0.912 (0.783, 0.961)
	Control	25.3 (18.7, 31.9)		
Mortise width	Clubfoot	26.0 (18.6, 33.3)	0.027	0.917 (0.838, 0.959)
	Control	27.5 (21.2, 33.9)		
Mortise/talus ratio	Clubfoot	1.13 (0.88, 1.38)	0.017	
	Control	1.09 (0.84, 1.33)		
Length	Clubfoot	42.0 (30.0, 54.1)	0.303	0.905 (0.817, 0.952)
	Control	43.1 (32.5, 53.7)		
Neck depth	Clubfoot	2.3 (0.7, 3.9)	< 0.001	0.869 (0.749, 0.934)
	Control	3.6 (2.0, 5.1)		
Neck angle	Clubfoot	126.6 (97.2, 156.1)	0.116	0.773 (0.489, 0.895)
	Control	122.5 (94.7, 150.4)		

CI indicates confidence interval; ICC, intraclass correlation coefficient; PACS, picture archiving and communication system.

correlation coefficients (ICCs) were suggestive of agreement. Inter-rater [2,1] reliability was as defined by Shrout et al.[15]

3D Model Measures

Average talus widths in our 3D models were 24 mm in controls and 22.8 mm in clubfeet ($P = 0.173$). Average mortise width was found to be 27.8 mm in controls versus 25.3 mm within the clubfoot cohort ($P = 0.014$). Model talus length was comparable in both groups with 44.9 mm in controls and 43 mm in clubfeet ($P = 0.212$). Talus neck depth was nearly identical to PACS-based measures with 2.3 mm in clubfeet and 3.5 mm in controls ($P = 0.003$). Talus neck angle was also significantly different at 140.4 degrees in controls and 153.7 in clubfeet ($P = 0.01$). Volume was 23391.5 and 21372.4 mm^3 in controls and clubfeet, respectively ($P = 0.185$). Tibial arc of curvature was 27.6 mm in controls compared with 28.0 mm in clubfeet (0.882). Talus arc was 18.0 mm in controls with an average radius of 18.7 mm in clubfeet ($P = 0.562$).

DISCUSSION

The Ponseti method of clubfoot correction (serial casting and heel cord tenotomy) has become the international standard of care for the initial treatment of the idiopathic clubfoot. Despite this, a certain number of patients will have residual deformity that may require surgical reconstruction to improve foot position, balance, and function. Many of these children will have residual equinus deformity that may respond to surgical Z-lengthening of the Achilles tendon and appropriate release of the posterior ankle and subtalar joints. Yet despite adequate release, in the senior author's experience; intraoperative release of these structures can occasionally fail to substantially improve dorsiflexion. In these cases, it seems that abnormal articular morphology could be a cause and thus soft tissue surgical release could be unlikely to gain the desired motion. The purpose of the current study was to determine if there could be articular incongruities or morphologic differences that could account for residual equinus. We used MRI to assess ankle shape as these children are toddlers with a large amount of unossified cartilage that would be difficult to appreciate on radiographs or CT images.

Before this study, several anatomic variations of the clubfoot talus had already been described with the use of MRI and/or modeling. In 1988, Herzenberg et al[6] used histologic sections of a single clubfoot to generate a 3D computer model. This model was found to have a talar neck that was internally rotated relative to the mortise with a body that was externally rotated to this same reference point. It should be noted that our measures were obtained differently, do not intend to address medialization, and are instead looking purely at depth and plantarflexion across the neck of the talus. As a result our novel measuring techniques could neither truly agree or disagree with Herzenberg and colleagues.

In 2000, Kamegaya et al[11] examined MRI data from 21 subjects (31 total ankles) including both operative (17) and nonoperative cases after Ponseti casting (14). When compared with age-matched controls the talar neck was found to be medially deviated as suggested by prior literature. The unique finding by Kamegaya and colleagues was a lack of difference between the operative and nonoperative groups looking at this same variable. A more recent study (2004) from Itohara et al was based on MRI data from 5 patients following serial casting.[9] This data were used to produce 3D models via a marching cubes method that was quite different from our own. This study reported smaller talus volumes with medial deviation of the talar head and neck. Plantar deviation was not found to be significant.

There is still much to be learned regarding the reasons for residual equinus and inadequate surgical correction of equinus. One of our initial hypotheses for residual equinus was the possibility that the anterior talus was simply too wide to fit within the mortise, blocking dorsiflexion. If this were the case, then surgical release of the syndesmosis could potentially improve the situation. From this data we documented smaller talus widths (23.2 vs. 25.3 mm) and mortise widths (26 vs. 27.5 mm) in clubfeet, consistent with their hypoplastic nature. The observed mortise ratio was slightly greater in clubfeet in comparison to normal feet (1.13 vs. 1.09, respectively); thus arguing against increased talus width and the need for syndesmosis release.

Another limitation to motion could be the possibility of flattened or incongruent sagittal arc of curvature of the talus and tibia. It is well known that older clubfeet can have a flat-topped appearance noted on radiographs (Fig. 4) and thus soft tissue releases would not be expected to improve dorsiflexion. In these cases, guided growth of the distal tibia, distal tibial osteotomy or talus removal or decancelization could be indicated. From our 3D modeling, we learned that there was no significant difference in the sagittal arc of the talus or the corresponding tibia. Another cause of decreased dorsiflexion could be impingement of the talus neck on the anterior edge of the distal tibial articular

FIGURE 4. Lateral radiograph of the foot in a 6-year-old boy with residual equinus after the Ponseti method and posterior release at age 4. The flat-topped articular incongruity of the talus in relation to the tibia would seem to suggest an inability to dorsiflex further as a result of articular flattening.

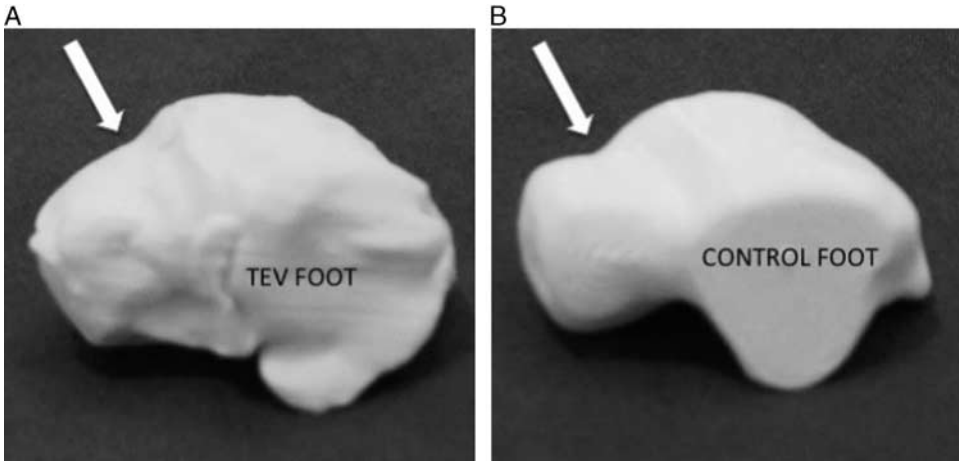

FIGURE 5. Actual 3D models printed from a child with unilateral clubfoot (A). In comparison to his normal foot (B); the clubfoot model has much less neck offset and could be likely to impinge on the anterior edge of the distal tibia joint and restrict dorsiflexion.

surface that limits dorsiflexion. Data from this study appears to support this hypothesis.

Novel parameters measured directly from PACS MRI data assessed possible impingement by documenting the talus neck depth and neck angle. This analysis did reveal significant differences in talus depth for clubfeet in comparison with control feet at 2.3 and 3.6 mm, respectively (<0.001). There was an insignificant trend toward less acute neck angle in clubfeet in comparison with control feet when assessed directly on MRI. 3D model-based measures however, did produce a significantly larger neck angle in clubfeet versus control feet (153.7 vs. 140.4 degrees, respectively; $P=0.01$). 3D modeling also confirmed a significantly decreased talus neck depth in clubfeet with residual equinus deformity in comparison with control feet at 2.3 and 3.5 mm, respectively ($P=0.003$). Although we reported preoperative dorsiflexion (Table 1) for completion, we would be remised to include a comparison or correlation to talar neck depth or angle in our study. Our preoperative dorsiflexion measures were not standardized and reported via the electronic medical record by a single observer.

As far as we are aware, this data is the first description of a shallow talar neck in toddlers with residual clubfoot deformity (Fig. 5). It is possible that decreased neck depth is present at birth, serving as a source of limited dorsiflexion in this population. Alternatively, decreased ankle motion may be the root problem preventing normal cartilage remodeling of the talar neck. Regardless of etiology, we believe that a shallow talar neck could result in sagittal plane impingement, reducing intraoperative dorsiflexion despite complete lengthening and release of posterior ankle contracture. In addition, we no longer perform syndesmosis release as there does not appear to be evidence for coronal plane impingement as a result of mismatch in talus to mortise width. Even though we are often unable to gain desirable intraoperative dorsiflexion after soft tissue release; we have observed gradual improvement in dorsiflexion with use of stretching AFO's and physiotherapy (unpublished observations). Perhaps this would imply the talus neck could deepen with time and through the process of skeletal maturation improve ankle dorsiflexion as a result of decreased impingement.

Limitations

The primary focus of this study was to determine sources of residual equinus, or more accurately, decreased dorsiflexion in surgical clubfoot patients. With that in mind, one possible limitation in this retrospective study is the absence of forced dorsiflexion MRIs. Casting in forced dorsiflexion would potentially allow one to avoid/limit sedation, however it would be unlikely to have changed our sectioning methods or raw data. We cautiously state above that we believe sagittal plane impingement may be a source of decreased dorsiflexion in some cases and would not consider this lone publication a testament to that conclusion.

In this study we chose to evaluate ankle morphology with MRI scans and made measures from the scans directly; as well as from computer generated models of the same data. The later methodology has the advantage to average for potential variability between different slice thickness and orientation of the slices. Comparison between the 2 methods demonstrated good reproducibility and just a few discrepancies were noted. There are several potential reasons for these differences with the most obvious being human error in the data extraction process. Each step in processing required human intervention to identify the borders of the talus, to refine the masks and stl files, and lastly to make the measures themselves. Another contribution could be the obligatory divergence in reference point measures due to the constraints imposed by slice thickness on PACS measures. As stated above, these neck angle measures could not be made precisely at the chosen equidistant points, while they could on our 3D models.

Sample size also impacted this study and our ability to assess for differences both within and between cohorts. Areas for future investigation might include differences between feet in unilateral patients as well as age dependent differences

(across the 2 to 6 y old spectrum) within the clubfoot cohort itself. Our statistician simply did not feel that our group sizes were large enough to make accurate comparisons.

The retrospective nature of this publication also prevented us from comparing our MRI findings to established clubfoot severity scales such as Dimeglio and Pirani scores. Although we did have a documented Pirani score for a for a subset of our patients, these were recorded at the time of initial casting. Recurrence and resultant surgery occurred at least 2 years later. Similarly, objective postoperative dorsiflexion measures were only available for 7 of 17 patients, limiting our ability for comparison.

CONCLUSIONS

Anterior ankle impingement may be a component of residual equinus deformity in toddlers with clubfeet who were treated in the manner of Ponseti. With MRI data we have noted a decrease in the talar neck depth and a more obtuse talar neck angle in comparison to normal age-matched feet. When performing posterior release in these patients, the treating surgeon should recognize this possibility when the amount of dorsiflexion obtained after release appears to less than what one would expect. Although not tested in this manuscript; it is hoped that remodeling and improved dorsiflexion could be gained with prolonged stretching and use of a stretching AFO.

REFERENCES

1. Docquier PL, Leemrijse T, Rombouts JJ, et al. Clinical and radiographic features of operatively treated stiff clubfeet after skeletal maturity: etiology of the deformities and how to prevent them. *Foot Ankle Int*. 2006;1:29–37.
2. Morcuende J, Hosseinzadeh P, Kiebzak GM, et al. Management of clubfoot relapses with the ponseti method: results of a survey of the POSNA Members. *J Pediatr Orthop*. 2017. [Epub ahead of print].
3. Epeldegui T. Deformity of talus and calcaneous in congenital clubfoot: an anatomical study. *J Pediatr Orthop*. 2012;1:10–15.
4. Farsetti P, De Maio F, Russolillo L, et al. CT study on the effect of different treatment protocols for clubfoot pathology. *Clin Orthop Relat Res*. 2009;5:1243–1249.
5. Johnson CE, Hobatho MC, Baker KJ, et al. Three-dimensional analysis of clubfoot deformity by computed tomography. *J Pediatr Orthop*. 1995;4:39–48.
6. Herzenberg JE, Carroll NC, Christofersen MR, et al. Clubfoot analysis with three-dimensional computer modeling. *J Pediatr Orthop*. 1988;8:257–262.
7. Shapiro F, Glimcher MJ. Gross and histlogical abnormalities of the talus in congenital clubfoot. *J Bone Joint Surg*. 1979;61:522–530.
8. Windisch G, Anderhuber F, Haldi-Brandle V, et al. Anatomical study for an update comprehension on clubfoot. Part I: bones and joints. *J Child Orthop*. 2007;1:69–77.
9. Itohara T, Sugamoto K, Shimizu N, et al. Assessment of talus deformity by three-dimensional MRI in congenital clubfoot. *Eur J Radiol*. 2005;1:78–83.
10. Downey DJ, Drennan JC, Garcia JF. Magnetic resonance image findings in congenital talipes equinovarus. *J Pediatr Orthop*. 1992;12:224–228.
11. Kamegaya M, Shinohara Y, Kokuji Y, et al. Evaluation of pathologic abnormalities of clubfoot by magnetic resonance imaging. *Clin Orthop*. 2000;83:726–730.
12. Irani RN, Sherman MS. The pathologic anatomy of idiopathic clubfoot. *Clin Orthop*. 1972;84:14–20.
13. Wang C, Petursdottir S, Leifsdottir I, et al. MRI multiplanar reconstruction in the assessment of congenital talipes equinovarus. *Pediatr Radiol*. 1999;29:262–267.
14. Ippolito E. Update on pathologic anatomy of clubfoot. *J Pediatr Orthop*. 1995;4:17–24.
15. Shrout PE, Fleiss JL. Intraclass correlations: uses in assessing rater reliability. *Psychol Bull*. 1979;86:420–428.